CERN-INTC-2021-038 / INTC-I-232
12/05/2021

EUROPEAN ORGANIZATION FOR NUCLEAR RESEARCH

Letter of Intent to the ISOLDE and Neutron Time-of-Flight Committee

Collinear laser spectroscopy of selenium isotopes

May 12, 2021

X. F. Yang[1], L. V. Rodríguez[2,3], S. W. Bai[1], M. L. Bissell[4], K. Blaum[3], B. Cheal[5], R. F. Garcia Ruiz[6], T. Lellinger[2,7], S. Malbrunot-Ettenauer[2], R. Neugart[3,8], G. Neyens[9], W. Nörtershäuser[7], R. Sánchez[10], S. J. Wang[1], D. T. Yordanov[11].

[1]*School of Physics and State Key Laboratory of Nuclear Physics and Technology, Peking University, Beijing, China*
[2]*Experimental Physics Department, CERN, Geneva, Switzerland*
[3]*Max-Planck-Institut für Kernphysik, Heidelberg, Germany*
[4]*School of Physics and Astronomy, The University of Manchester, Manchester, United Kingdom*
[5]*Oliver Lodge Laboratory, University of Liverpool, United Kingdom*
[6]*Massachusetts Institute of Technology, Cambridge, MA 02139, USA*
[7]*Institut für Kernphysik, Technische Universitat Darmstadt, Darmstadt, Germanyy*
[8]*Institut für Kernchemie, Universitat Mainz, Mainz, Germany*
[9]*Instituut voor Kern- en Stralingsfysica, KU Leuven, Leuven, Belgium*
[10]*GSI Helmholtzzentrum für Schwerionenforschung GmbH, Darmstadt, Germany*
[11]*Université Paris-Saclay, CNRS/IN2P3,IJCLab, 91405 Orsay, France*

Spokesperson: X.F. Yang, xiaofei.yang@pku.edu.cn
Co-spokesperson: L. V. Rodríguez, liss.vazquez.rodriguez@cern.ch
Contact person: L. V. Rodríguez, liss.vazquez.rodriguez@cern.ch

Abstract: We propose to measure ground- and isomeric-state properties of Se ($Z = 34$) isotopes across the $N = 40$ and $N = 50$ (sub)shell closures using high-resolution collinear laser spectroscopy. The aim is to study the structural evolution from single-particle to deformation around $N = 40$, and the level evolution above $N = 50$. The production of Se isotopes around $N = 40$ are available at ISOLDE, however, we have learned from our previous experience in Ge (IS623) that the beam contaminants are very complex. This letter of intent aims to investigate the level of (possible molecular) contamination by performing a preliminary measurement of the six stable isotopes and of four radioactive species at the COLLAPS setup. This will help us to investigate the possible effect on the experimental sensitivity and will motivate beam developments for more exotic cases. In addition, it will shed light on the origin of the sudden drop of the nuclear size of ^{74}Se.

Requested shifts: 5 shifts of radioactive beam and 3 shifts of stable beam.

1 Introduction

High-resolution collinear laser spectroscopy is a powerful tool to measure ground and isomeric state properties of nuclei across the nuclear landscape. These properties include the nuclear spins, electromagnetic moments and mean-square charge radii, which can help us understand various aspects of the nuclear structure. For instance in the Ni ($Z = 28$) region, several experiments performed at ISOLDE [1, 2, 3, 4, 5, 6] have provided valuable information on the study of shell evolution [7, 4], the magic effect of $N = 40$ and $N = 50$ [8, 9] and nuclear deformation [10, 11, 5]. Around $N = 40$ in particular, measurements of nuclear charge radii and moments have indicated that the weak sub-shell effect observed at $N = 40$ in Ni isotopes disappears quickly as protons are added to the $Z = 28$ closed shell [2, 3], and structural changes occur from the single-particle nature of Ni to deformation in Ge [5]. On the other hand, around the $N = 50$ neutron magic number, shape coexistence has been reported in ^{79}Zn ($N = 49$) [10] and the level evolution of $1/2^+$ and $5/2^+$ of the $N = 51$ isotones (between $Z = 28$ and $Z = 40$) has been predicted theoretically and indicated experimentally [6].

Located in the middle between the two proton closed (sub)shells $Z = 28$ and $Z = 40$, the

Table 1: Known information of the ground-state properties (spins, magnetic and quadrupole moments, charge radii) of Se isotopes ($Z = 34$) from literature [12, 13, 14, 15, 16, 17] and the reported production yields at ISOLDE using a ZrO_2 target[18, 19].

Isotopes	half-life	spins	μ (μ_N)	Q(b)	$\delta\langle r^2\rangle$	Yield (ions/μC)
^{69}Se	27.4 s	$1/2^-$	—	—	—	
^{71}Se	4.74 m	$(5/2^-)$	—	—	—	4.0×10^5
^{73}Se	7.15 h	$9/2^+$	0.892(13)	—	—	$<3.0\times10^8$
^{73m}Se	39.8 m	$3/2^-$	—	—	—	$<3.0\times10^8$
^{75}Se	119.8 d	$5/2^+$	0.683(10)	1.2578(6)	—	2.4×10^8
^{77}Se	stable	$1/2^-$	+0.5350422(6)	—	✓	
^{77m}Se	17.36 s	$7/2^+$	—	—	—	
^{79}Se	3.3x10^5 y	$7/2^+$	-1.018(15)	+0.8(2)	—	
^{79m}Se	3.92m	$1/2^-$	—	—	—	
^{81}Se	18.45 m	$1/2^-$	—	—	—	$<2.1\times10^5$
^{81m}Se	57.28 m	$7/2^+$	—	—	—	$<2.1\times10^5$
^{83}Se	22.3 m	$9/2^+$	—	—	—	$<3.9\times10^3$
^{83m}Se	70.1 s	$1/2^-$	—	—	—	$<3.9\times10^3$
^{85}Se	32.9 s	$(5/2^+)$	—	—	—	
^{70}Se	41.1 m	0^+	—	—	—	2.0×10^5
^{72}Se	8.40 d	0^+	—	—	—	3.0×10^8
^{74}Se	stable	0^+	—	—	✓	
^{76}Se	stable	0^+	—	—	✓	
^{78}Se	stable	0^+	—	—	✓	
^{80}Se	stable	0^+	—	—	✓	
^{82}Se	stable	0^+	—	—	✓	

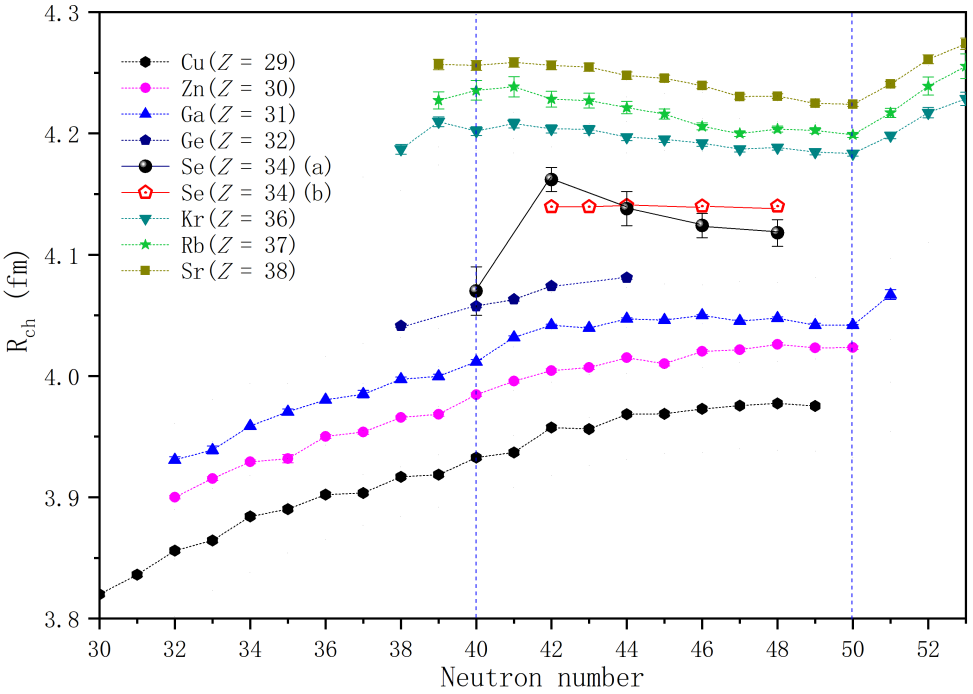

Figure 1: Root mean square charge radii in the Ni region [2, 3, 9, 20, 21, 16, 17]. It has to be noted that the charge radii of Se isotopes marked as Se(a) and Se(b) are extracted from electron scattering and muonic atom data, respectively [16, 17].

Se isotopes ($Z = 34$) contain rich nuclear structure information. Interesting phenomena such as shape coexistence [22, 23] and triaxial deformation [24] around $N = 40$, single particle structure around $N = 50$, as well as shape evolution in neutron rich isotopes [25] have been investigated using different approaches [22, 25, 26, 27]. Ground state properties of Se isotopes, would be of great value for such nuclear structure studies. However, as shown in Table 1, experimental information on nuclear moments and charge radii of Se is rare and mostly limited to stable or long-lived cases. This is probably due to the production difficulties of atomic selenium at ISOL facilities [19] and the limited information on the atomic structure of this element [28].

Figure 1 presents the nuclear charge radii in the Ni region, showing an enhanced collective effect around $N = 40$ with increasing Z. For heavier Kr, Rb and Sr isotopes, the charge radii continuously increase with decreasing neutron number from $N = 50$ to $N = 40$, indicating that a large deformation appears around $N = 40$. The known charge radii of the six stable Se isotopes, calculated from electron scattering and muonic atom data, are included in Fig. 1 and marked with Se(a) and Se(b), respectively [16, 17]. Although only limited data is available and (unlike radii determined from laser spectroscopy) the values are model dependent, a similar trend is observed for Se from $N = 48$ to $N = 40$. This trend is very different from that of Ge, Ga, Zn and Cu isotopes. It has to be noted that a sudden drop of charge radii is found for ^{74}Se ($N = 40$). With the current data and the systematic in the region, it is impossible to answer whether this sudden change comes from a change in the structure of ^{74}Se or from a measurement problem. Therefore, an independent measurement of the charge radii along the Se isotopic chain by

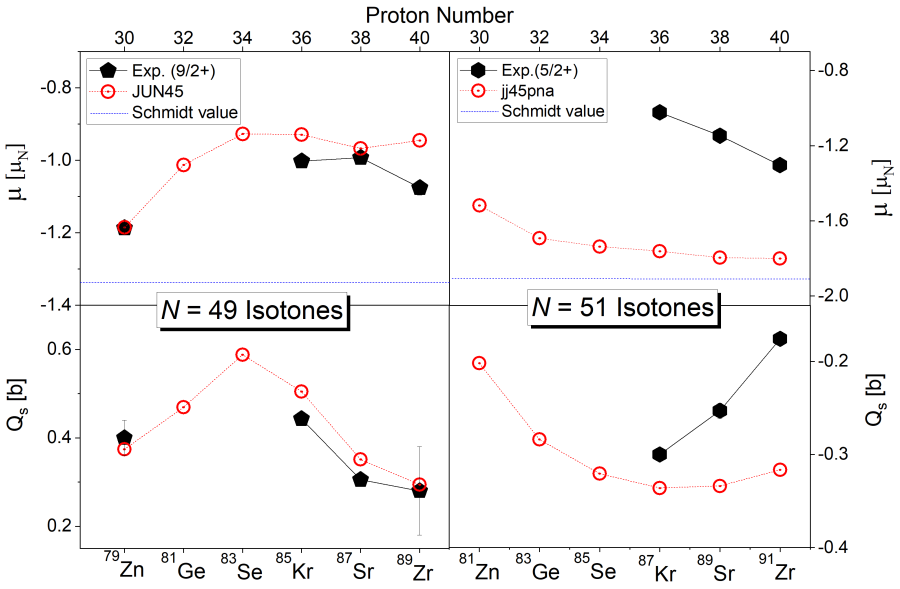

Figure 2: Experimental nuclear magnetic and quadrupole moments of $N = 49$ and $N = 51$ isotones [10, 29] below proton semi-magic number of $Z = 40$ compared with the shell-model calculations using JUN45 and jj45pna interactions, respectively.

high-resolution laser spectroscopy is necessary. These together with the electromagnetic moments will be of particular importance for the investigation of nuclear shapes of Se isotopes around $N = 40$.

At $N = 50$, a clear magic shell effect is seen from the charge radii of heavier Kr, Rb, Sr isotopes. However, as discussed above, experimental investigation has shown that different exotic structural phenomena appear around $N = 50$ at different proton numbers, e.g. around $Z = 28$, shape coexistence was found in ^{79}Zn [10] and ^{78}Ni [30]. It is thus worth to studying the ground state properties of Se isotopes around $N = 50$, just in the middle of $Z = 28$ and $Z = 40$, which will allow the $Z-$dependence of the structure to be investigated. Figure 2 shows the available data on magnetic and quadrupole moments of $N = 49$ and $N = 51$ isotones [10, 29], which are compared with simple shell-model calculations. The parabolic trend of the nuclear moments of $N = 49$ isotones predicted by the shell model is in line with the energy systematics (see Fig. 4 in Ref. [10]). The known experimental moments follow reasonably the predicted trend. The experimental measurement of nuclear moments of ^{81}Ge (proposed in an earlier letter of intent (LOI) [31]) and ^{83}Se (this LOI) nuclides will enrich our understanding of the structural trend in the $N = 49$ isotonic sequence. For the $N = 51$ isotones, the energy gap of $1/2^+$ and $5/2^+$ states is predicted to be reduced and then inverted (see Fig. 1 in Ref. [6]) with decreasing Z from 40 to 28. We can thus expect that the configuration mixing of the ground state wave functions of $N = 51$ isotones will be enhanced towards $Z = 28$, which is consistent with the trend of nuclear moments predicted by the shell-model (Fig. 2). The known experimental moments (Fig. 2) seem to follow the predicted general trend but with the limited experimental data conclusions can not be made. More experimental moments of ^{83}Ge (earlier LOI [31]) and ^{85}Se (this LOI) are required to study the level evolution and possible inversion in $N = 51$ isotones [6].

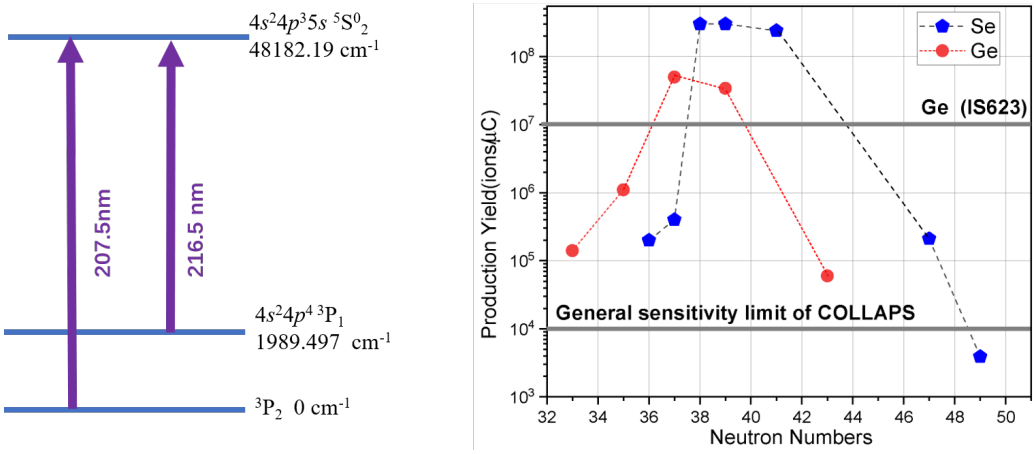

Figure 3: Left: Laser schemes of selenium atoms used for collinear laser spectroscopy measurement [19, 28]. Right: Reported production yield of germanium isotopes [31] and selenium isotopes using a ZrO_2 target [18]. The two horizontal gray lines indicate the general sensitivity limit ($\sim 10^4$ ions/s) of COLLAPS and the experimental sensitivity ($> 10^7$ ions/s) of the laser spectroscopy measurement of germanium isotopes due to the large contamination and unknown molecules in the beams.

2 Experimental method

The ground- and isomeric-state properties of Se isotopes will be studied using the collinear laser spectroscopy technique with fluorescence detection at the COLLAPS set-up [32, 5]. The bunched ion beam released from ISCOOL will be neutralized using a charge exchange cell filled with potassium vapor to populate the atomic state of interest. The charge exchange process of Se ions with potassium vapor has been simulated [33] and the $^3P_1$ state is expected to be well populated. We will perform laser spectroscopy measurements of the hyperfine structures (HFS) and isotope shifts using the $4s^24p^4\ ^3P_1 \rightarrow 4s^24p^35s\ ^5S^0_2$ transition (216.5 nm) shown in Fig. 3 (left). This wavelength can be accessed by frequency quadrupling of the Matisse laser, as has been and will be used for different COLLAPS experiments (IS497, IS635, IS667) [34, 35, 36].

From our previous measurements in Ge (IS623), we have learned that a huge amount of contaminants appear at each mass including the stable ones (without mass markers). That significantly limited the experimental sensitivity of COLLAPS to 10^7 ions/s (shown in Fig. 3 (right)) which is generally around 10^4 ions/s, as has been well demonstrated from other experiments [32]. In addition, a heavier mass component was observed in the time of flight (TOF) spectrum of bunched germanium beams, as shown in Fig. 4 and detailed in Ref. [5]. It is known that the radioactive ion beam produced in this region using a ZrO_2 target contains molecular components [18, 19]. However, such molecular beams released from the target can not be transported to COLLAPS after the high resolution mass separator. Thus, a natural guess would be that the heavier mass component observed in the TOF spectrum (Fig. 4) is a molecular contamination formed in the ISCOOL. However, we have no information on how the molecular contamination is formed, and what element it contains. Investigating this phenomena will be crucial for laser spectroscopy experiments, and would potentially be of interest for other users/experiments at ISOLDE.

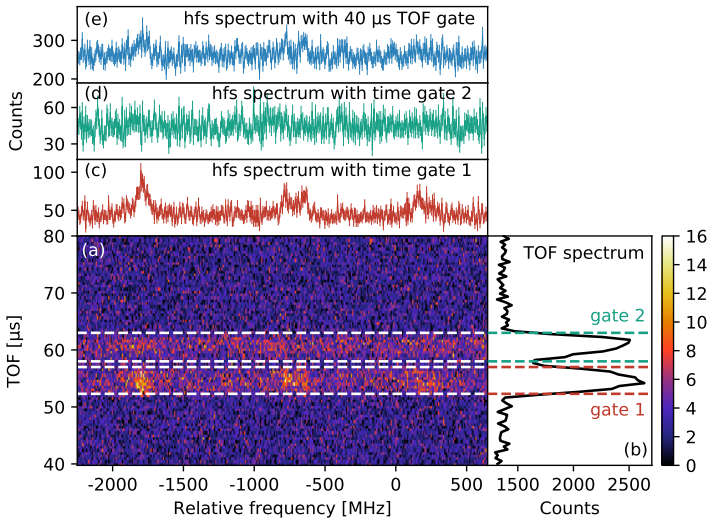

Figure 4: Time of flight spectrum together with the associated hyperfine structure spectrum of ^{73}Ge measured from COLLAPS experiment on germanium isotopes. The two components presented in the TOF spectrum are corresponding to the germanium bunch (gate 1 in red) and the possible molecular contamination bunch (gate 2 in green). Figure is taken from Ref. [5].

Therefore, in order to measure the nuclear properties of neutron-deficient and neutron-rich Se isotopes at COLLAPS, before submitting a full proposal, **we would like to verify the following information with a preliminary online measurement:**

1. The experimental sensitivity of COLLAPS for a HFS spectrum measurement with pure stable Se isotopes from mass markers on the proposed atomic transition (Fig. 3 (left)) .
2. The levels of isobaric contamination in the radioactive Se beam, which will limit the performance of the ISCOOL and COLLAPS.
3. The molecular contamination formed in the ISCOOL, which can be assessed by measuring the TOF spectrum and fluorescence counts at COLLAPS, as shown in Fig. 4.

As shown in Fig. 3 (right) and Table 1, the reported production yields of four unstable Se isotopes are larger than 10^8 ions/s, which is already higher than the experimental sensitivity reached in the germanium experiment at COLLAPS (IS623). Additionally, there are six stable Se isotopes available which can be provided as pure ion beam. Therefore, with this letter of intent, we aim to measure the HFS spectra of more than 10 states of Se isotopes.

3 Required beam development

From the ISOLDE online yield database, Se beams have only been produced using PSB and a ZrO_2 target but, as mentioned above, it is known that large molecular contaminations are present in the beam. A recently developed RILIS ionization scheme has succeed in producing ^{71}Se with a promising yield [19]. But, as noted in Ref. [19], further developments of RILIS for identifying transitions to auto-ionizing states are required to improve the laser ionization efficiency. In addition, beam development from UC_x target for the

production of neutron-rich Se isotopes above $N = 50$ are requested with this letter of intent.

4 Beam-time request

Selenium has six stable isotopes. A preliminary laser spectroscopy measurement of these isotopes would already provide valuable (model-independent) data for the nuclear charge radii, which will help us to figure out the origin of the sudden drop of the nuclear size of ^{74}Se, as shown in Fig. 1. Therefore, we request 3 shifts of stable beam to measure the HFS spectra of stable $^{74,76-78,80,82}$Se. One shift of the stable isotope ^{80}Se will be used before the experiment to optimize the set-up, and to evaluate the experimental sensitivity with the pure beam. This information will be important for the assessment of the contamination and its effect on the experimental sensitivity once radioactive Se isotopes are measured.

Assuming that the laser spectroscopy measurement of radioactive Se isotopes is at the same level of sensitivity as our previous Ge experiment (IS623), we could perform the HFS spectra measurement of ^{72,73,73m,75,79}Se isotopes with the production yield of $> 10^7$ ions/s. Therefore, we request four shifts of radioactive ^{72,73,73m,75,79}Se beams for the contamination assessment and for the HFS spectra measurements, as summarized in Table 2. For ^{70,71,81,81m}Se with production yields of $\sim 10^5$ ions/s, we probably can not reach sufficient sensitivity due to the unknown information of the contamination. We thus request one shift to evaluate the level of (possible molecular) contamination using the RFQ and the COLLAPS setup.

Summary of requested shifts:
3 shifts of stable beam for the optimization of the setup and charge radii measurement of stable isotopes. 5 shifts of radioactive beams for the contamination assessment and online measurement.

Table 2: Summary of the requested beam time for the contamination assessment and for laser spectroscopy measurements.

Isotopes	Yield (ions/μC)	Contamination assessment /physics case	shifts
^{70}Se	2.0×10^5	Contamination	1
^{71}Se	4.0×10^5		
^{81,81m}Se	2.1×10^5		
^{72}Se	3.0×10^8	Contamination/physics	0.5
^{73,73m}Se	3.0×10^8	Contamination/physics	1.5
^{75}Se	2.4×10^8	Contamination/physics	1
^{79}Se	Long-lived	Contamination/physics	1
$^{74,76-78,80,82}$Se	stable	Charge radii measurement	2
^{80}Se	stable	Preparation	1

References

[1] S. Kaufmann, J. Simonis, S. Bacca, J. Billowes, M. L. Bissell, K. Blaum, B. Cheal, R. F. Garcia Ruiz, W. Gins, C. Gorges, G. Hagen, H. Heylen, A. Kanellakopoulos, S. Malbrunot-Ettenauer, M. Miorelli, R. Neugart, G. Neyens, W. Nörtershäuser, R. Sánchez, S. Sailer, A. Schwenk, T. Ratajczyk, L. V. Rodríguez, L. Wehner, C. Wraith, L. Xie, Z. Y. Xu, X. F. Yang, and D. T. Yordanov. Charge radius of the short-lived ^{68}Ni and correlation with the dipole polarizability. *Phys. Rev. Lett.*, 124:132502, Apr 2020.

[2] M. L. Bissell, T. Carette, K. T. Flanagan, P. Vingerhoets, J. Billowes, K. Blaum, B. Cheal, S. Fritzsche, M. Godefroid, M. Kowalska, J. Krämer, R. Neugart, G. Neyens, W. Nörtershäuser, and D. T. Yordanov. Cu charge radii reveal a weak sub-shell effect at N= 40. *Physical Review C*, 93:064318, Jun 2016.

[3] L. Xie, X.F. Yang, C. Wraith, C. Babcock, J. Bieroń, J. Billowes, M.L. Bissell, K. Blaum, B. Cheal, L. Filippin, K.T. Flanagan, R.F. Garcia Ruiz, W. Gins, G. Gaigalas, M. Godefroid, C. Gorges, L.K. Grob, H. Heylen, P. Jönsson, S. Kaufmann, M. Kowalska, J. Krämer, S. Malbrunot-Ettenauer, R. Neugart, G. Neyens, W. Nörtershäuser, T. Otsuka, J. Papuga, R. Sánchez, Y. Tsunoda, and D.T. Yordanov. Nuclear charge radii of $^{62-80}$Zn and their dependence on cross-shell proton excitations. *Physics Letters B*, 797:134805, 2019.

[4] B. Cheal, E. Mané, J. Billowes, M. L. Bissell, K. Blaum, B. A. Brown, F. C. Charlwood, K. T. Flanagan, D. H. Forest, C. Geppert, M. Honma, A. Jokinen, M. Kowalska, A. Krieger, J. Krämer, I. D. Moore, R. Neugart, G. Neyens, W. Nörtershäuser, M. Schug, H. H. Stroke, P. Vingerhoets, D. T. Yordanov, and M. Žáková. Nuclear spins and moments of ga isotopes reveal sudden structural changes between N= 40 and N= 50. *Phys. Rev. Lett.*, 104:252502, Jun 2010.

[5] A. Kanellakopoulos, X. F. Yang, M. L. Bissell, M. L. Reitsma, S. W. Bai, J. Billowes, K. Blaum, A. Borschevsky, B. Cheal, C. S. Devlin, R. F. Garcia Ruiz, H. Heylen, S. Kaufmann, K. König, Á. Koszorús, S. Lechner, S. Malbrunot-Ettenauer, R. Neugart, G. Neyens, W. Nörtershäuser, T. Ratajczyk, L. V. Rodríguez, S. Sels, S. J. Wang, L. Xie, Z. Y. Xu, and D. T. Yordanov. Nuclear moments of germanium isotopes near $N = 40$. *Physical Review C*, 102:054331, Nov 2020.

[6] M. Athanasakis, S. W. Bai, S. Bester, et al. Probing the magicity and shell evolution in the vicinity of $N = 50$ with high-resolution laser spectroscopy of ^{81,82}Zn isotopes. *(CERN-INTC-2020-064 ; INTC-P-579)*, Sep. 2020.

[7] K. T. Flanagan et al. Nuclear spins and magnetic moments of ^{71,73,75}Cu: inversion of the $\pi 2p_{3/2}$ and $\pi 1f_{5/2}$ levels in ^{75}Cu. *Physical Review Letters*, 103:142501, 2009.

[8] C. Wraith et al. Evolution of nuclear structure in neutron-rich odd-Zn isotopes and isomers. *Physics Letters B*, 771:385–391, 2017.

[9] R. P. de Groote, J. Billowes, C. L. Binnersley, M. L. Bissell, T. E. Cocolios, T. D. Goodacre, G. J. Farooq-Smith, D. V. Fedorov, K. T. Flanagan, S. Franchoo, et al. Measurement and microscopic description of odd–even staggering of charge radii of exotic copper isotopes. *Nature Physics*, 16:620–624, 2020.

[10] X. F. Yang et al. Isomer shift and magnetic moment of the long-lived $1/2^+$ isomer in $^{79}_{30}Zn_{49}$: signature of shape coexistence near ^{78}Ni. *Physical Review Letters*, 116:182502, 2016.

[11] X. F. Yang et al. Investigating the large deformation of the $5/2^+$ isomeric state in ^{73}Zn: an indicator for triaxiality. *Physical Review C*, 97:044324, 2017.

[12] I. Berkes, R. Hassani, and M. Massaq. Ground state spin and magnetic moment of ^{73}Se. *Physical Review C*, 38:2329–2331, Nov 1988.

[13] L. C. Aamodt and P. C. Fletcher. Spin, quadrupole moment, and mass of selenium-75. *Phys. Rev.*, 98:1224–1229, Jun 1955.

[14] H. E. Weaver. Magnetic moments of ^{29}Si, ^{33}S, ^{67}Zn, ^{75}As, ^{77}Se, ^{123}Te, and ^{125}Te. *Phys. Rev.*, 89:923–930, Mar 1953.

[15] W. A. Hardy, G. Silvey, C. H. Townes, B. F. Burke, M. W. P. Strandberg, George W. Parker, and Victor W. Cohen. The nuclear moments of ^{79}Se. *Phys. Rev.*, 92:1532–1537, Dec 1953.

[16] I. Angeli and K.P. Marinova. Table of experimental nuclear ground state charge radii: An update. *Atomic Data and Nuclear Data Tables*, 99(1):69–95, 2013.

[17] G. Fricke and K. Heilig. Nuclear charge radii in "elementary particles, nuclei and atoms". Springer-Verlag Berlin Heidelberg.

[18] U. Köster, U.C. Bergmann, D. Carminati, R. Catherall, J. Cederkäll, J.G. Correia, B. Crepieux, M. Dietrich, K. Elder, V.N. Fedoseyev, L. Fraile, S. Franchoo, H. Fynbo, U. Georg, T. Giles, A. Joinet, O.C. Jonsson, R. Kirchner, Ch. Lau, J. Lettry, H.J. Maier, V.I. Mishin, M. Oinonen, K. Peräjärvi, H.L. Ravn, T. Rinaldi, M. Santana-Leitner, U. Wahl, and L. Weissman. Oxide fiber targets at isolde. *Nuclear Instruments and Methods in Physics Research B*, 204:303–313, 2003.

[19] K. Chrysalidis, J. Ballof, Ch. E. Düllmann, V. N. Fedosseev, C. Granados, B. A. Marsh, Y. Martinez Palenzuela, J. P. Ramos, S. Rothe, T. Stora, and K. Wendt. Developments towards the delivery of selenium ion beams at isolde. *The European Physical Journal A*, 55:173, 2019.

[20] T. J. Procter, J. Billowes, M. L. Bissell, K. Blaum, F. C. Charlwood, B. Cheal, K. T. Flanagan, D. H. Forest, S. Fritzsche, Ch. Geppert, H. Heylen, M. Kowalska, K. Kreim, A. Krieger, J. Krämer, K. M. Lynch, E. Mané, I. D. Moore, R. Neugart, G. Neyens, W. Nörtershäuser, J. Papuga, M. M. Rajabali, H. H. Stroke, P. Vingerhoets, D. T. Yordanov, and M. Žáková. Nuclear mean-square charge radii

of $^{63,64,66,68-82}$Ga nuclei: No anomalous behavior at $N=$ 32. *Physical Review C*, 86:034329, Sep 2012.

[21] G. J. Farooq-Smith, A. R. Vernon, J. Billowes, C. L. Binnersley, M. L. Bissell, T. E. Cocolios, T. Day Goodacre, R. P. de Groote, K. T. Flanagan, S. Franchoo, R. F. Garcia Ruiz, W. Gins, K. M. Lynch, B. A. Marsh, G. Neyens, S. Rothe, H. H. Stroke, S. G. Wilkins, and X. F. Yang. Probing the $_{31}$Ga ground-state properties in the region near $Z=$ 28 with high-resolution laser spectroscopy. *Physical Review C*, 96:044324, Oct 2017.

[22] K. Wimmer, W. Korten, P. Doornenbal, T. Arici, P. Aguilera, A. Algora, T. Ando, H. Baba, B. Blank, A. Boso, S. Chen, A. Corsi, P. Davies, G. de Angelis, G. de France, J.-P. Delaroche, D. T. Doherty, J. Gerl, R. Gernhäuser, M. Girod, D. Jenkins, S. Koyama, T. Motobayashi, S. Nagamine, M. Niikura, A. Obertelli, J. Libert, D. Lubos, T. R. Rodríguez, B. Rubio, E. Sahin, T. Y. Saito, H. Sakurai, L. Sinclair, D. Steppenbeck, R. Taniuchi, R. Wadsworth, and M. Zielinska. Shape changes in the mirror nuclei ^{70}Kr and ^{70}Se. *Phys. Rev. Lett.*, 126:072501, Feb 2021.

[23] J. H. Hamilton, A. V. Ramayya, W. T. Pinkston, R. M. Ronningen, G. Garcia-Bermudez, H. K. Carter, R. L. Robinson, H. J. Kim, and R. O. Sayer. Evidence for coexistence of spherical and deformed shapes in ^{72}Se. *Phys. Rev. Lett.*, 32:239–243, Feb 1974.

[24] G. H. Bhat, W. A. Dar, J. A. Sheikh, and Y. Sun. Nature of γ deformation in Ge and Se nuclei and the triaxial projected shell model description. *Physical Review C*.

[25] S. Chen, P. Doornenbal, A. Obertelli, et al. Low-lying structure and shape evolution in neutron-rich Se isotopes. *Physical Review C*, 95:041302, Apr 2017.

[26] D. T. Doherty, J. Ljungvall, M. Zielińska, et al. Probing shape coexistence in neutron-deficient ^{72}Se via low energy coulomb excitation. *(CERN-INTC-2014-057 / INTC-P-423)*, October 2014.

[27] C. Lizarazo, P.-A. Söderström, V. Werner, et al. Metastable states of ^{92,94}Se: Identification of an oblate k isomer of ^{94}Se and the ground-state shape transition between $n = 58and60$. *Phys. Rev. Lett.*, 124:222501, Jun 2020.

[28] D. A. Gillett, S. J. Diggines, and J. M. Brown. Measurement of the fine structure splittings of atomic Se and Sn in their ground 3p states. *Phys. E: AI. Mol. Opt, phys.*, 27(21):5175–5184, nov 1994.

[29] T.J. Mertzimekis, K. Stamou, and A. Psaltis. An online database of nuclear electromagnetic moments. *Nuclear Instruments and Methods in Physics Research Section A: Accelerators, Spectrometers, Detectors and Associated Equipment*, 807:56–60, 2016.

[30] R. Taniuchi, C. Santamaria, P. Doornenbal, et al. ^{78}Ni revealed as a doubly magic stronghold against nuclear deformation. *Nature*, 569:53–58, 2019.

[31] M. L. Bissell, X. F. Yang, J. Billowes, et al. Ground and isomeric state spins, moments and radii of Ge isotopes across the $N = 40$ subshell closure via laser spectroscopy at collaps. *(CERN-INTC-2016-035 / INTC-P-472)*, June 2016.

[32] R. Neugart, J. Billowes, M. L. Bissell, K. Blaum, B. Cheal, K. T. Flanagan, G. Neyens, W. Nörtershäuser, and D. T. Yordanov. Collinear laser spectroscopy at ISOLDE: new methods and highlights. *Journal of Physics G: Nuclear and Particle Physics*, 44(6):064002, apr 2017.

[33] A. R. Vernon, J. Billowes, C. L. Binnersley, M. L. Bissell, T. E. Cocolios, G. J. Farooq-Smith, K. T. Flanagan, R. F. Garcia Ruiz, W. Gins, R. P. de Groote, Á. Koszorús, K. M. Lynch, G. Neyens, C. M. Ricketts, K. D. A. Wendt, S. G. Wilkins, and X. F. Yang. Simulation of the relative atomic populations of elements $1 \leq Z \leq 89$ following charge exchange tested with collinear resonance ionization spectroscopy of indium. *Spectrochimica Acta Part B: Atomic Spectroscopy*, 153:61–83, 2019.

[34] D. T. Yordanov, K. Blaum, D. L. Balabanski, et al. Laser spectroscopy of cadmium isotopes towards $N = 50$. *(CERN-INTC-2012-023 / INTC-P-271-ADD-1)*, January 2012.

[35] Z.Y. Xu, D.T. Yordanov, D.L. Balabanski, et al. Nuclear quadrupole moments and charge radii of the $_{51}$Sb isotopes via collinear laser spectroscopy. *(CERN-INTC-2017-010 / INTC-CLL-028)*, January 2017.

[36] L.V. Rodríguez, S Bai, M. L. Bissell, et al. Laser spectroscopy of neutron-rich tellurium isotopes. *(CERN-INTC-2020-036 / INTC-P-561)*, May 2020.

Appendix

DESCRIPTION OF THE PROPOSED EXPERIMENT

The experimental setup comprises: (*name the fixed-ISOLDE installations, as well as flexible elements of the experiment*)

Part of the	Availability	Design and manufacturing
COLLAPS	☒ Existing	☒ To be used without any modification

HAZARDS GENERATED BY THE EXPERIMENT Hazards named in the document relevant for the fixed COLLAPS installation.